Cu-based alloys as a benchmark for T-PGAA quantitative analysis at spallation neutron sources

L. Arcidiacono[a,b,c], M. Martinón-Torres[d], R. Senesi[a,c,e*], A. Scherillo[f], C. Andreani[a,c], G. Festa[c]

[a]Universita' degli studi di Roma Tor Vergata, NAST Centre and Physics Department, viale della Ricerca Scientifica 1, Rome, Italy
[b]UCL Institute of Archaeology 31-34 Gordon Square, London, UK
[c]CENTRO FERMI - Museo Storico della Fisica e Centro Studi e Ricerche "Enrico Fermi", piazza del Viminale 1, Rome, Italy
[d]Department of Archaeology, University of Cambridge, Downing Street, Cambridge UK
[e]CNR-IPCF Sezione di Messina, Viale Ferdinando Stagno d'Alcontres 37, Messina, 98158 Italy
[f]STFC-ISIS pulsed neutron and muon source, Rutherford Appleton Laboratory, Harwell Oxford, Didcot, UK

Abstract

In this paper, we present the quantitative analysis carried out for the first time using time-resolved prompt gamma activation analysis (T-PGAA), a recent technique currently under development at ISIS Neutron and Muon Source in Oxfordshire. T-PGAA is a neutron technique based on the radiative capture reaction that allows the simultaneous acquisition of the photon energy emitted by the object during irradiation, and the time of flight of the neutron that starts the capture reaction. We discuss results from two Cu-based certified standards from MBH Analytical Ltd: a leaded bronze and a brass, in preparation for future applications such as archaeological copper alloys. Results show the validity of the quantitative analysis calculated through the new data analysis software developed in-house for this technique through comparison with the certified values and XRF results.

Keywords: Cu alloys, ROOT software, PGAA, NRCA, Quantitative analysis, HPGe

1. Introduction

Time-resolved prompt gamma activation analysis (T-PGAA) is an innovative neutron technique currently under development at ISIS pulsed Neutron and Muon Source. A protocol analysis was developed and tested on a set of copper-based standards. An Ortec high-purity germanium GMX40P4-76RB detector has been used to acquire simultaneously the photon-energy promptly emitted by the irradiated object and the time at which the prompt gamma-ray has been detected. This bi-parametric acquisition allows to build a bi-dimensional matrix where the prompt gamma energy is represented as a function of the neutron time of flight (TOF), which is directly related to the neutron energy that emitted the prompt gamma.

*Prof. Roberto Senesi: roberto.senesi@uniroma2.it

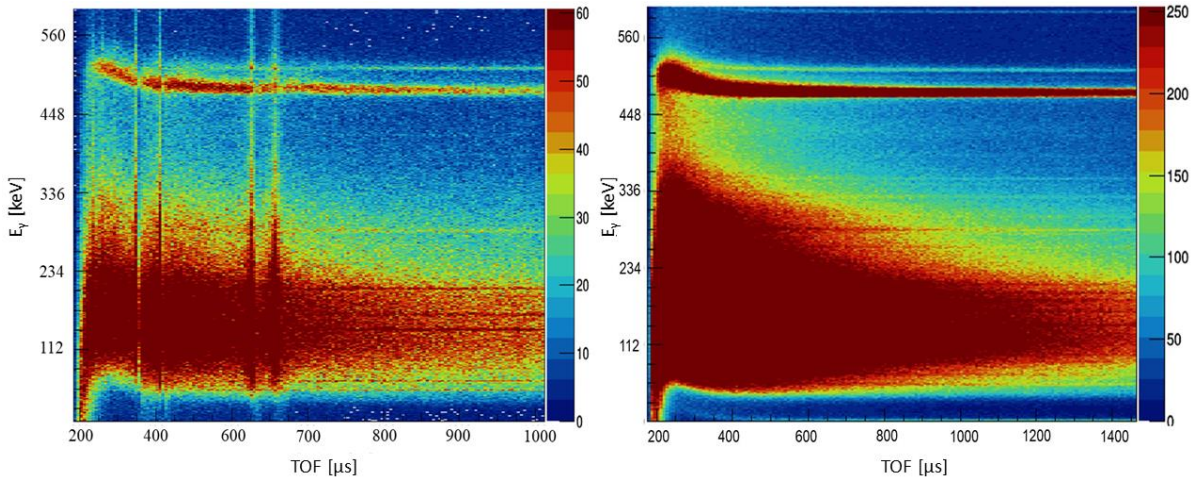

Figure 1: *The bidimensional matrix representing the γ-energy vs the time of flight of the absorbed neutron that produces gammas from the leaded bronze (on the left) and the brass standards (on the right). From this representation it is possible to appreciate the resonances in time of flight as well as some of the characteristics of the gamma spectra such as the annihilation peak at 511 keV.*

This bi-dimensional matrix allows to select ranges in the x-axis corresponding to the TOF directly related to the neutron energy, and make projections on the γ-axis corresponding to the γ-energy. In T-PGAA technique the TOF is the difference between the time at which the gamma is detected by the germanium detector and the proton synchrotron time-pulse that generates the neutron flux with a frequency of 50 Hz. This technique allows an enhanced sensitivity in the investigation of major, minor and trace elements within an object [1-5].

Neutron techniques for the characterisation of objects of different materials have been successfully used for long time at reactors and at spallation sources [1, 6]. Neutrons are appropriate for the study of metal objects, for which a variety of techniques is available for chemical characterisation as well as for microstructural studies and lattice properties identification [1, 7-11]. Prompt gamma activation analysis (PGAA) and neutron resonance capture analysis (NRCA) are among the most fruitful techniques for the isotopic characterisation of a high variety of materials (e.g. metals, ceramics, stones). They are both based on the radiative capture reaction where the incident neutron hits a target nucleus, that in turn gets activated and emits prompt gamma rays during irradiation. PGAA has been developed mainly at reactors [2, 12] and reveals the gamma energy spectrum of the photons emitted by the sample, while NRCA, developed at the linear accelerator GELINA, reveals the neutron TOF spectrum of resonances isotopically selective for each chemical element through the acquisition of the emitted gamma [13, 14]. A different probe that is routinely used and considered effective for the characterisation of metal objects are X-rays-based techniques such as x-ray fluorescence spectroscopy (XRF). XRF is a valuable technique for the detection of the elemental composition of the investigated sample [15], but the area excited and analysed is restricted to the surface of the sample.

The aim of this paper is to present the quantitative analysis tailored for time-resolved prompt gamma activation analysis developed and tested at ISIS spallation Neutron and Muon Source on INES beamline. In particular, we aim at comparing the quantitative results on two certified Cu-based obtained through T-PGAA technique with the certified values provided by the company and XRF results, in order to assess the potential of the technique and the validity of the data analysis procedure and in-house software that enable to quantify the elements identified within the samples. [16] Results show that T-PGAA technique and the *ad hoc* developed software and procedure for data analysis can quantify major and minor elements with high accuracy for all elements investigated, except for zinc ,

*Prof. Roberto Senesi: roberto.senesi@uniroma2.it

as shown below This methodology can be applied for the bulk analysis of materials in general, with particular potential for ancient objects due to the non-invasive nature of the technique.

2. Experimental

We studied two cylindrical copper-based standards (Figure 2) supplied by the MBH Analytical Ltd: MBH 32X LB10 leaded bronze and MBH 31X B9 brass of 39.7 mm in diameter and 3.7 mm thickness [17] on INES beamline at ISIS Pulsed Neutron and Muon Source.

Figure 2: *Standards issued by the MBH Analytical LTD*

INES is a powder diffractometer usually devoted to the phase characterisation of objects, but due to the high epithermal flux that the beamline offers, it is also used to test new detectors and new types of setup [16, 18]. To acquire the signal, we positioned a high-purity germanium detector GMX40P4-RB, refrigerated through electric Ortec XCooler [19] at 77K, through one of the aluminium windows on INES tank, in forward scattering position. The output signal of the detector is sent to channel 1 of a Caen Digitizer DT5724 set to collect the energy of the gamma emitted by the sample during irradiation and the time at which this gamma has been revealed (t_i). Channel 2 of the digitizer is used to collect the T_0 of the synchrotron registering the time of each pulse. The channels are recorded on two ASCII files that are fed into a ROOT algorithm [20] that synchronises each pulse with the related t_i, calculates the TOF by ($T_0 - t_i$) and creates a bi-dimensional matrix where the photon energy is represented as a function of TOF. Through the software it is possible to study the influence of different ranges in TOF making cuts in the x-axis of the matrix and projecting on the y-axis to see the variations on gamma spectra. The management of these processes is left to customised ROOT scripts built and validated through calibrated gamma sources and the comparison with Hypermet PC [21-25]. The second part of data manipulation consists of the background subtraction, peaks identification, peak-fitting and efficiency correction [24-29].

The background has been experimentally obtained for each standard, removing the sample from the sample holder and leaving the remaining experimental conditions (i.e. jaws aperture, sample to detector distance, irradiation time, sample holder in place) not altered. During the off-line analysis the background and sample data were normalised to the live time. The background was then subtracted bin per bin from the sample data (see Figure 3). We acquired a background for each sample to be consistent with the experimental setup.

*Prof. Roberto Senesi: roberto.senesi@uniroma2.it

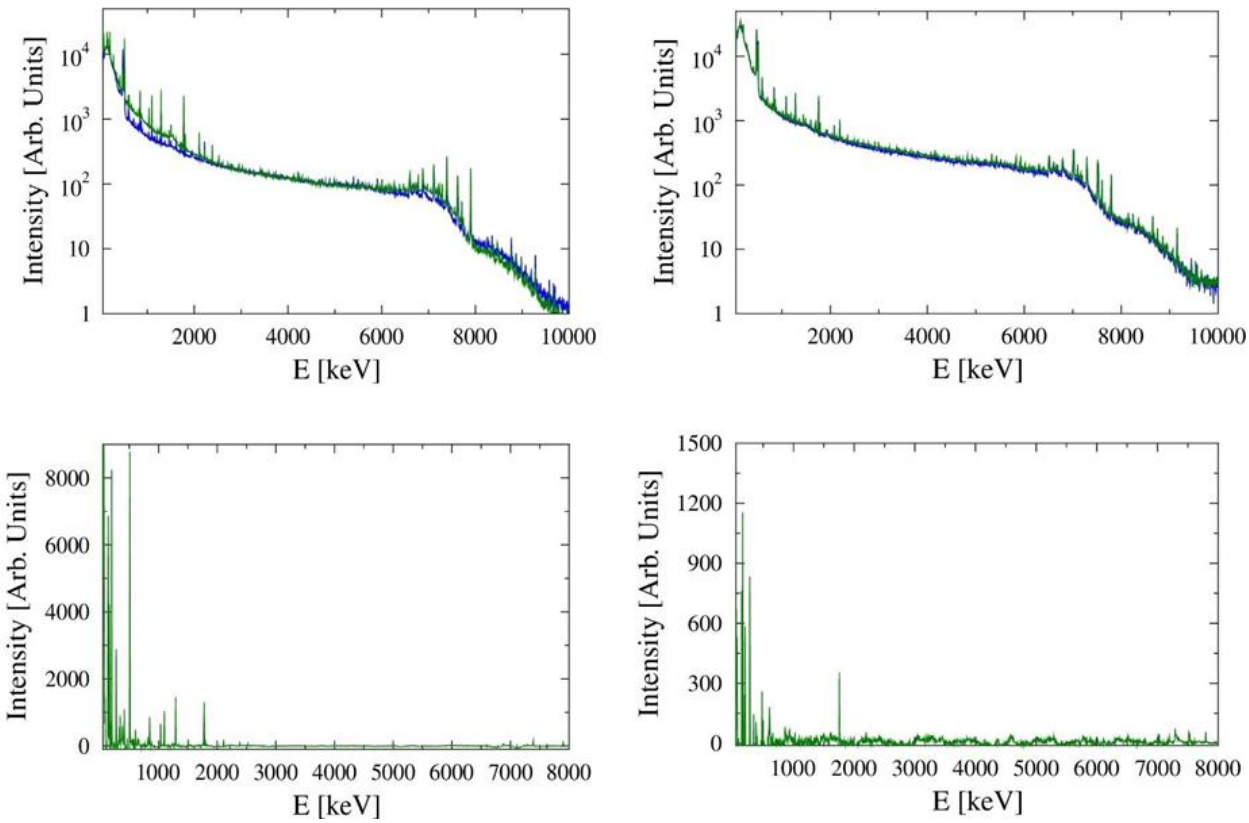

Figure 3: *Left: The upper figure represents the leaded bronze thermal cut (in green) and relative background in blue, while the lower figure is the signal from the leaded bronze standard after the background was removed. Right: the upper figure represents the brass thermal cut in green and related background in blue, while the bottom figure is the signal from the brass after the background was removed. We can notice that the brass sample remains noisier compared to the other and therefore the peak quantification might be imprecise.*

T-PGAA data are treated by doing cuts to select time of flight regions corresponding to the thermal and epithermal neutron energy ranges. The gamma spectrum from the neutron thermal contribution is used for qualitative and quantitative analysis. The total energy spectrum (thermal and epithermal components) is analysed making cuts in time of flight around the resonances of the tin (Sn, TOF = 212 – 368 µs that corresponds to E_n = 20 – 60 eV) and silver (Ag, TOF = 580 – 1166 µs that corresponds to E_n = 2 – 8 eV). We separate different neutron-energies to highlight different contributions in the gamma spectrum.

*Prof. Roberto Senesi: roberto.senesi@uniroma2.it

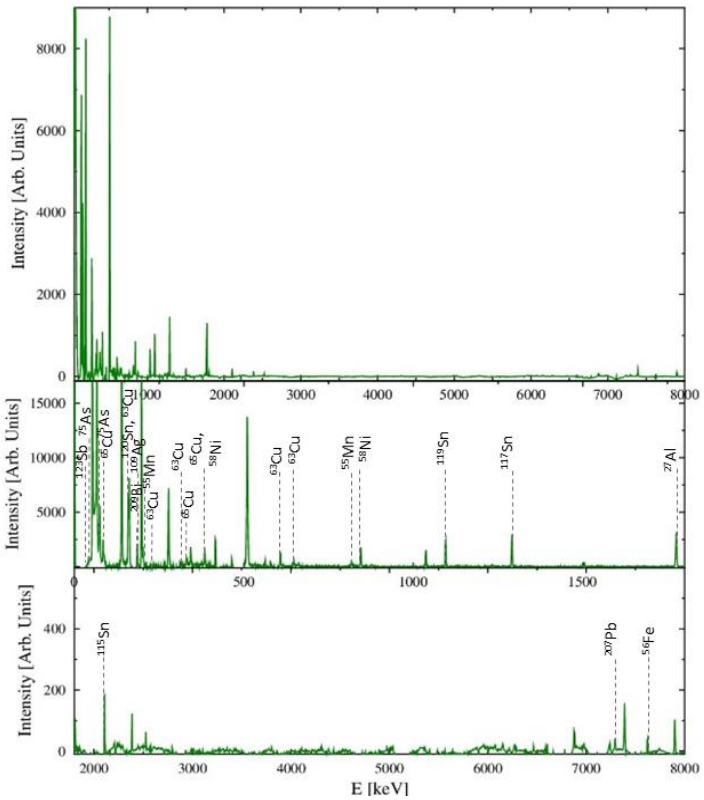

Figure 4: *Bronze γ spectrum obtained from the bi-dimensional matrix E_γ vs ToF in the thermal range of the x-axis.*the simultaneous acquisition of the photon-energy emitted by the object during irradiation, and the time of flight of the neutron that starts the capture reaction *The upper figure represents the entire energy range spanning from 50 keV to 8 MeV. The second and third plots are zooms into two different regions of the energy range, 50 keV to 2 MeV and 2 to 8 MeV respectively.*

The unlabelled peaks in figure 4 correspond to the sample-dependent background that cannot be entirely removed [24]. The standard metal samples were produced from commercial-purity metals, and master alloys. The discs are the product of one melt poured into a sequence of multiple chill moulds with feeding systems designed to ensure round discs. Each certified element has been analysed by several laboratories, and 95% half-width confidence intervals for the resultant mean values have been derived from methods such as inductively coupled plasma atomic emission spectroscopy (ICP-AES), atomic absorption spectrometry (AAS), and others. We focused on the analysis of Cu-based standard samples because of the interest in future archaeometric investigations.

3. Results and Discussion

To assess the validity of the new data analysis software, we made a comparison between percentages in weight calculated using the certified values and those calculated through the T-PGAA technique. Tables 1 and 2 report the peak characterisation of the gamma spectra for leaded bronze and brass standard samples. The first three columns describe the peak parameters of the fitting procedure for each identified gamma: the gamma energy (E_γ), the peak area (A) and the full width half maximum (FWHM). Columns from four to six display the isotopes identified through the comparison between the experimental E_γ and the corresponding value from the IAEA database [25]. In column five we also report the gamma cross section of each labelled isotope. From the comparison between the experimental γ-energy and the IAEA tabulated γ-energy, we can see that at higher energies we have some discrepancies mainly due to the conjunction of a low detection efficiency with the non-linearity correction implemented in the software [26].

*Prof. Roberto Senesi: roberto.senesi@uniroma2.it

Leaded Bronze thermal neutron energy contribution					
FWHM [keV]	**Area [cps]**	**Eγ [keV]**	**Isotopes**	**γ Cross Sect. [barns]**	**IAEA Eγ [keV]**
1.32 ± 0.02	1869.54 ± 15.47	41.19 ± 0.48	^{123}Sb	0.1	40.80 ± 0.05
2.23 ± 0.08	2910.58 ± 85.98	46.70 ± 0.35	^{75}As	0.33	46.09 ± 0.05
2.15 ± 0.05	17534.45 ± 593.57	74.80 ± 0.32	^{75}As	0.12	74.87 ± 0.05
2.15 ± 0.03	6978.69 ± 165.21	84.78 ± 1.35	^{65}Cu	0.1	89.08 ± 1.88
2.39 ± 0.02	20987.69 ± 425.48	159.6 ± 1.77	^{120}Sn; ^{63}Cu	0.01; 0.64	158.66 ± 0.29; 159.28 ±1.48
2.39 ± 0.01	22778.18 ± 95.14	161.87 ± 5.23	^{209}Bi	0.01	162.16 ± 3.15
2.58 ± 0.02	4202.96 ± 64.25	185.66 ± 1.65	^{65}Cu	0.24	185.96 ± 2.67
2.58 ± 0.02	44844.71 ± 415.05	198.16 ± 1.56	^{109}Ag	7.75	198.72 ± 0.54
3.02 ± 0.35	5248.05 ± 25.11	202.63 ± 0.65	^{63}Cu	0.19	202.95 ± 0.05
1.26 ± 0.02	588.33 ± 28.21	211.44 ± 2.54	^{55}Mn	2.13	212.04 ± 0.78
2.39 ± 0.02	18042.31 ± 140.22	277.82 ± 2.87	^{63}Cu	0.89	278.25 ± 1.05
2.58 ± 0.01	4662.21 ± 65.17	343.39 ± 1.75	^{63}Cu	0.22	343.89 ± 0.05
2.58 ± 0.03	4164.17 ± 8.26	384.63 ± 0.09	^{65}Cu	0.13	385.77 ± 2.67; 464.93 ± 1.47
2.58 ± 0.02	1593.03 ± 5.65	464.28 ± 1.03	^{65}Cu; ^{58}Ni	0.13; 0.84	465.14 ± 1.42; 464.97 ± 1.96
2.10 ± 0.11	1176.07 ± 42.01	578.46 ± 0.09	^{63}Cu	0.09	579 ± 0.02
2.89 ± 0.15	3444.43 ± 9.08	607.50 ± 0.32	^{63}Cu	0.27	608.77 ± 0.02
3.02 ± 0.02	1483.10 ± 3.51	647.48 ± 0.14	^{63}Cu	0.1	648.80 ± 0.05
2.58 ± 0.02	4557.54 ± 5.01	845.04 ± 1.05	^{55}Mn d	13.1	846.75 ± 0.03
2.58 ± 0.01	620.42 ± 20.09	876.48 ± 0.03	^{58}Ni	0.23	877.97 ± 0.03
2.58 ± 0.01	6384.85 ± 3.77	1170.91 ± 0.14	^{119}Sn	0.09	1171.28 ± 0.10
3.01 ± 0.01	8032.08 ± 8.94	1290.62 ± 6.45	^{117}Sn	0.13	1293.59 ± 0.02
2.58 ± 0.01	9198.03 ± 12.77	1775.18 ± 5.27	^{27}Al d	0.23	1778.92 ± 0.03
3.01 ± 0.38	1130.30 ± 16.32	2107.91 ± 3.01	^{115}Sn	0.02	2112.30 ± 0.09
4.54 ± 0.44	22.72 ± 1.32	7367.12 ± 3.01	^{207}Pb	0.13	7367.78 ± 0.09
4.58 ± 0.45	84.38 ± 6.34	7622.00 ± 3.01	^{56}Fe	0.65	7631.13 ± 0.12

Table 1: *Peak analysis of the PGAA from the thermal neutron energy contribution of the leaded bronze standard sample. The d displayed near some of the isotopes indicates that the signal is due to the delayed gammas rather than prompt gammas.*

*Prof. Roberto Senesi: roberto.senesi@uniroma2.it

Brass thermal neutron energy contribution					
FWHM [keV]	**Area [cps]**	**Eγ [keV]**	**Isotopes**	**γ Cross Sect. [barns]**	**IAEA Eγ [keV]**
0.55 ± 0.02	1406.64 ± 25.47	72.19 ± 0.45	^{109}Ag; ^{75}As	0.12; 0.90	74.87 ± 0.04; 72.67 ± 0.02
0.30 ± 0.08	225.01 ± 10.97	113.47 ± 0.19	^{64}Zn; ^{121}Sb	0.17; 0.40	115.22 ± 0.02; 114.54 ± 0.04
0.55 ± 0.03	2666.53 ± 54.30	144.30 ± 0.26	^{75}As	0.10	144.54 ± 0.05
0.30 ± 0.09	195.63 ± 25.67	149.25 ± 1.73	^{121}Sb	0.4	148.24 ± 1.59
0.55 ± 0.03	2655.45 ± 136.76	163.02 ± 1.23	^{209}Bi	0.01	162.19 ± 1.88
0.55 ± 0.02	597.63 ± 22.84	166.31 ± 0.67	^{75}As	0.99	165.05 ± 0.24
0.55 ± 0.02	732.49 ± 74.14	188.91 ± 2.33	^{65}Cu	0.24	185.96 ± 3.15
0.55 ± 0.01	1828.30 ± 56.32	201.50 ± 1.05	^{63}Cu	0.19	202.95 ± 2,46
0.55 ± 0.02	468.96 ± 10.02	207.01 ± 1.23	^{107}Ag	3.58	206.46 ± 0.54
0.16 ± 0.36	95.03 ± 3.44	235.85 ± 0.65	^{75}As; ^{109}Ag	0.18; 4.62	235.87 ± 0.24; 235.62 ± 0.53
0.55 ±0.01	2341.74 ± 438.21	280.16 ± 2.75	^{63}Cu	0.89	278.25 ± 0.78
0.55 ± 0.02	307.44 ± 30.22	345.00 ± 2.87	^{63}Cu	0.21	343.89 ± 1.05
0.41 ± 0.22	231.16 ± 22.74	384.62 ± 1.75	^{65}Cu	0.13	385.67 ± 0.05
0.53 ± 0.03	133.62 ± 3.26	463.67 ± 0.09	^{65}Cu; ^{58}Ni	0.13; 0.84	465.14 ± 0.09; 464.93 ± 0.12
0.55 ± 0.02	476.62 ± 6.02	607.20 ± 1.03	^{63}Cu	0.27	608.76 ± 0.05
0.23 ± 0.13	80.69 ± 12.01	647.35 ± 0.09	^{63}Cu	0.1	648.80 ± 0.02
0.25 ± 0.15	19.38 ± 8.03	834.05 ± 0.32	^{68}Zn	0.04	834.77 ± 0.30
0.55 ± 0.02	186.07 ± 3.51	846.49 ± 0.14	^{55}Mn d	13.1	846.75 ± 0.05
0.55 ± 0.01	140.43 ± 5.74	1076.92 ± 1.05	^{68}Zn	0.35	1077.33 ± 0.03
0.54 ± 0.02	46.44 ± 3.09	1229.22 ± 0.03	^{117}Zn	0.07	1229.64 ± 0.07
0.55 ± 0.01	817.84 ± 7.35	1726.90 ± 0.14	^{56}Fe	0.18	1725.28 ± 0.03
0.55 ± 0.01	19.08 ± 4.32	6792.73 ± 4.21	^{31}P	0.03	6785.50 ± 0.05
0.55 ± 0.02	105.27 ± 3.24	7292. ± 6.45	^{56}Fe	0.13	7278.83 ± 0.03
0.55 ± 0.01	85.15 ± 7.63	7626.52 ± 5.27	^{56}Fe	0.65	7631.13 ± 0.05
1.05 ± 0.27	31.43 ± 3.32	7647.41 ± 3.01	^{56}Fe	0.55	7645.54 ± 0.05

Table 2: *Peak analysis of the PGAA from the thermal neutron energy contribution of the brass standard sample. The d displayed near some of the isotopes indicates that the signal is due to the delayed gammas rather than prompt gammas.*

Quantitative analyses of the T-PGAA spectra were calculated after subtracting the background, normalising the spectra to the live time and applying the efficiency corrections as explained in [26]. Then we summed all the peak areas from the isotopes of the same chemical element through the spectrum and normalised each of them for the irradiated area (in our case, a neutron beam of 3x3 cm^2 which covered the entire object). We took the result from the most abundant element, Cu in the case of the analysed standard samples, normalised for the known wt% provided by the certificates and scaled the other elements consequently as reported in [24]. Following Molnar method, we made the hypothesis that the volume of the standard samples irradiated by INES neutron flux corresponds to the quantity of the major element certified by the industry.

*Prof. Roberto Senesi: roberto.senesi@uniroma2.it

Leaded bronze				
	T-PGAA wt%	*Certificate wt%*	*Δ wt% (TPGAA - Certif)*	*XRF wt%*
Cu	77.23	77.23 ± 0.1	-	79.0 ± 0.2
Sn	7.31	8.26 ± 0.05	0.95	6.76 ± 0.03
Ag	0.01	0.05 ± 0.01	0.03	< LOD
Mn	4.67 d	-	-	< LOD
Ni	0.53	0.69 ± 0.01	0.16	0.71 ± 0.01
Al	0.01	0.020 ± 0.001	0.01	< LOD
Pb	11.02	12.46 ± 0.10	1.44	9.31 ± 0.04
As	0.11	0.150 ± 0.002	0.04	< LOD
Bi	0.07	0.060 ± 0.001	0.01	< LOD
Sb	0.69	0.560 ± 0.005	0.13	0.16 ± 0.03

Brass				
	T-PGAA wt%	*Certificate wt%*	*Δ wt% (TPGAA - Certif)*	*XRF wt%*
Cu	94.80	94.81 ± 0.07	-	94.33 ± 0.02
Zn	0.01	4.92 ± 0.04	4.91	5.19 ± 0.01
Sn	0.09	0.060 ± 0.002	0.02	0.45 ± 0.01
Fe	0.02	0.040 ± 0.001	-	0.003 ± 0.004
Ni	0.03	0.040 ± 0.001	0.01	< LOD
Al	< LOD	0.00	-	< LOD
Pb	< LOD	0.090 ± 0.003	-	0.03 ± 0.02
As	0.03	0.0100 ± 0.0003	0.02	< LOD
Te	< LOD	0.020 ± 0.001	-	< LOD
Bi	0.007	0.0060 ± 0.0002	0.001	< LOD
Se	0.001	0.0020 ± 0.0001	0.001	< LOD
P	0.001	0.0050 ± 0.0005	0.003	< LOD
Ag	0.006	0.0060 ± 0.0005	0.001	< LOD
Mn	0.670 d	0.0006 ± 0.0001	-	< LOD
Sb	0.005	0.0090 ± 0.0005	0.004	< LOD

Table 3: *Comparison between the quantitative results expressed in wt% for each element identified in the T-PGAA spectra, the certified values of the two MBH standard metal samples, and the XRF results. Concerning the T-PGAA results, for manganese the Mn d is the delayed signal. The quantitative values are reported considering an error of 0.01 except for the elements from Bi to the Sb in the brass table, which are elements present in traces, but well visible in the spectra due to their high gamma cross section. We present the quantitative analysis of these elements for comparison with the certified value, knowing that for real objects the calculation would be more difficult to attempt with such precision.*

Table 3 reports results for the leaded bronze and brass standard samples compared with those from the certified values. The relative distance between the quantitative values obtained respectively from the experimental (T-PGAA) and theoretical (certificates) data are reported in Table 3 as Δwt%. For comparison, XRF results are also considered. Looking at the comparison between the certificates and T-PGAA we notice that, for the leaded bronze, the major alloying constituents tin and lead are in agreement with the reference values within 1% while the error for minor and trace elements is 0.1% or, typically, much less. For the brass, results for trace elements show very good accuracy, within 0.02% of the reference values. We note, however, a mis-quantification for the major element zinc this standard, with our value of 0.01% largely underestimating a certified value of 4.92%. This is likely to be an effect of the background subtraction procedure: the INES beamline has zinc in its background and therefore it is likely that the signal from the background was higher that from the sample, and it was almost entirely removed from the spectrum through background subtraction. This kind of issue might be reduced or solved using an anticoincidence chain through which to operate Compton suppression coupled with a collimator. It is worth highlighting that in the bronze standard we were able to obtain a reliable quantification of lead, an element which is normally not easy to detect because of its low neutron cross section which determines, in turn, a low probability of interaction between the neutron and the lead nucleus. In this case, we could detect it because of its higher concentration within the sample (12.46%), compared to the brass standard (0.09%), where if fell below our detection limits. Further work will be needed with additional samples to establish the detection limits for this element. Concerning the minor elements listed in the certificates, T-PGAA could detect them all qualitatively and they also show good accordance quantitatively.

Through the comparison between T-PGAA and XRF we can observe that the first can quantify a larger number of elements, particularly because of its higher sensitivity and generally lower detection limits. In addition, XRF is based on x-rays, which in metals reach a depth of just tens or hundreds of micrometres while neutrons can reach a depth of several centimetres; thus, T-PGAA offers a true bulk composition, which is important in archaeological samples that may show surface alterations. Comparing T-PGAA and XRF with the certified quantitative values, we demonstrate the validity and the improvement of our technique in terms of sensitivity of elemental identification and

*Prof. Roberto Senesi: roberto.senesi@uniroma2.it

quantification, while we acknowledge the need to improve the detection of zinc. In the case of real objects of unknown composition, prior to any quantitative analysis, it is necessary to irradiate a standard sample with a similar composition and apply the same kind of normalisation described, i.e. normalising the quantitative results for the major element of the standard sample to match the relative certificate. Results after carrying out cuts in the ranges around tin and silver resonances as indicated above, and projecting in the y-axis, are reported in Figure 5 and table 4.

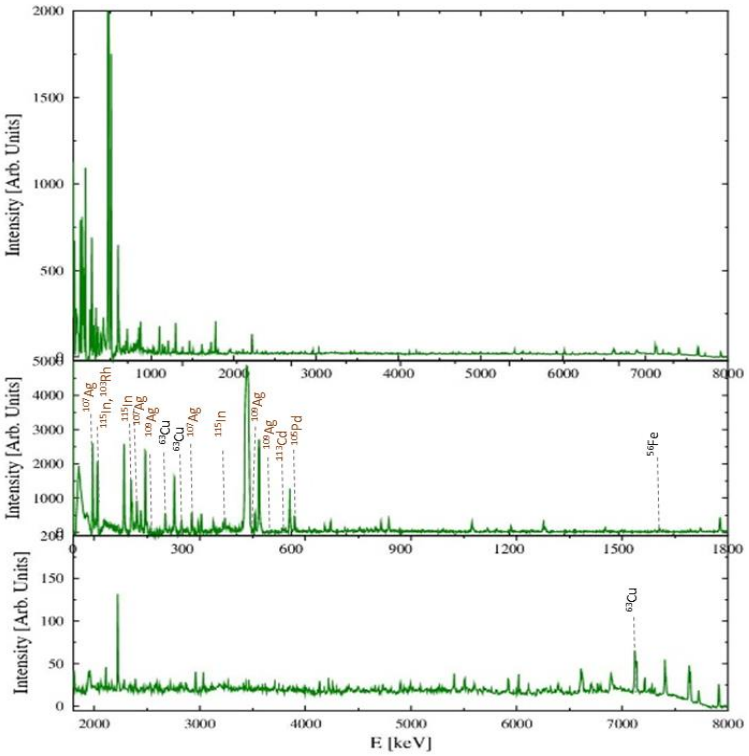

Figure 5: *Gamma energy spectra of the leaded bronze sample obtained making TOF cuts in around the ^{109}Ag resonance, and the labelling for isotope identification is also shown. The upper figure represents the entire energy range spanning from 50 keV to 8 MeV. The second and third plots are zooms in two different regions of the energy range, 50 keV to 2 MeV and 2 to 8 MeV respectively.*

Table 4 reports the peak characterisation of the gamma spectra for leaded bronze and brass standard samples in Sn and Ag resonances respectively. Columns one to three describe the peak parameters for each identified gamma energy: the gamma energy (E_γ), the peak area (A) and the full width half maximum (FWHM). Columns from four to six display the isotopes identified through the comparison between the experimental E_γ and the corresponding value from the IAEA database. In column five we also report the gamma cross section of each labelled isotope. Peaks highlighted in grey are those emerging after the in-resonance cuts. They are interpreted as daughter isotopes of tin and silver respectively; we also observe many delayed gammas due to the deactivation of these isotopes generally observable through neutron activation analysis (NAA) carried out at reactors.

Overall, T-PGAA is shown as an application of great potential for material characterisation because it allows to exploit time of flight resonance of a specific element of interest to investigate the spectra in more depth and unveil contributions that are otherwise hidden in the background. This application gains its maximum impact when applied for the investigation of minor and trace elements useful to determine the purity of a material for industrial purposes, or to investigate the provenance of archaeological metals in a non-destructive and non-invasive way. While the poor sensitivity for zinc will hinder the application of this method to archaeological brasses until this issue is resolved, it is

*Prof. Roberto Senesi: roberto.senesi@uniroma2.it

worth noting that zinc-bearing alloys only appear in the archaeological record from the first millennium BC, while all the prehistoric copper alloys from the preceding millennia are virtually zinc-free; furthermore, zinc in trace levels is not a good tracer for provenance, given its volatility and hence loss when metals are melted. Hence, prehistoric copper alloys appear as suitable artefacts for bulk chemical analyses employing this technique.

	LEADED BRONZE					
	FWHM [keV]	Area [cps]	E_γ [keV]	Isotope	Cross Section [barns]	IAEA E_γ [keV]
^{116}Sn resonance ToF = 212 – 368 μs E_n = 20 – 60 eV	0.56 ± 0.02	116.68 ± 9.33	279.85 ± 0.48	^{63}Cu	0.89	278.25 ± 0.03
	0.56 ± 0.09	35.01 ± 1.75	386.37 ± 0.35	^{115}In	12.10	385.11 ± 0.02
	0.57 ± 0.05	28.18 ± 1.41	415.47 ± 0.32	^{115}In d	43.00	416.86 ± 0.05
	0.38 ± 0.11	12.35 ± 0.62	564.37 ± 2.75	^{121}Sb d	2.70	564.24 ± 1.59
	0.30 ± 0.03	7.77 ± 0.38	692.21 ± 1.35	^{121}Sb d	0.15	692.65 ± 0.08
	0.56 ± 0.01	6.06 ± 0.25	721.73 ± 1.77	^{123}Te	0.52	722.77 ± 0.24
	0.56 ± 0.01	18.54 ± 1.38	856.76 ± 5.23	^{66}Zn	0.07	855.69 ± 0.15
	0.36 ± 0.02	12.65 ± 1.25	921.03 ± 1.65	^{121}Sb	0.08	921.01 ± 0.05
	0.56 ± 0.02	6.04 ± 0.30	1172.63 ± 1.56	^{119}Sn	0.09	1171.28 ± 0.54
	0.35 ± 0.03	2.61 ± 0.13	1232.32 ± 0.65	^{117}Sn	0.07	1229.64 ± 3.15
	0.50 ± 0.02	6.00 ± 0.30	1296.11 ± 2.54	^{115}Sn	0.13	1293.59 ± 0.78
	0.47 ± 0.02	4.55 ± 0.23	1339.27 ± 2.87	^{67}Zn	0.05	1340.14 ± 1.05
	0.25 ± 0.02	7.28 ± 0.44	1507.01 ± 1.75	^{115}In d	15.50	1507.40 ± 0.05
^{109}Ag resonance ToF = 580 – 1166 μs E_n = 2 – 8 eV	3.44 ± 0.02	996.36 ± 8.26	78.58 ± 0.09	^{107}Ag	3.90	78.90 ± 0.02
	1.11 ± 0.01	267.52 ± 5.65	84.80 ± 1.03	^{103}Rh	3.20	85.19 ± 0.05
	4.97 ± 0.11	3214.45 ± 122.01	160.71 ± 0.09	^{120}Sn; ^{63}Cu	0.014; 0.64	158.66 ± 0.05; 159.28 ± 0.02
	2.23 ± 0.15	491.71 ± 9.08	205.55 ± 0.32	^{107}Ag	3.58	206.46 ± 0.02
	0.52 ± 0.02	35.98 ± 2.16	265.25 ± 0.14	^{109}Ag	2.73	267.08 ± 0.05
	0.56 ± 0.02	76.33 ± 4.58	285.43 ± 1.05	^{115}In	4.50	284.91 ± 0.03
	0.56 ± 0.01	47.63 ± 2.38	298.21 ± 0.03	^{107}Ag	1.15	299.95 ± 0.03
	0.54 ± 0.01	29.42 ± 1.47	331.74 ± 0.14	^{103}Rh	3.27	333.44 ± 0.03
	0.56 ± 0.01	155.64 ± 7.78	344.01 ± 4.21	^{63}Cu	0.22	343.89 ± 0.05
	0.56 ± 0.01	172.97 ± 8.64	384.73 ± 6.45	^{65}Cu	0.13	385.77 ± 0.03
	1.67 ± 0.01	331.58 ± 5.57	416.43 ± 5.27	^{115}In d	43.00	416.86 ± 0.05
	0.56 ± 0.03	138.60 ± 2.92	465.07 ± 0.14	^{65}Cu, ^{58}Ni	0.13; 0.84	465.14 ± 0.06; 464.97 ± 0.04
	0.56 ± 0.03	58.60 ± 2.93	493.52 ± 2.25	^{109}Ag	1.08	495.71 ± 0.05
	0.56 ± 0.03	51.16 ± 1.87	579.46 ± 0.35	^{63}Cu	0.09	579.75 ± 0.05
	0.56 ± 0.03	38.25 ± 2.93	616.34 ± 0.17	^{105}Pd	0.62	616.19 ± 0.05
	0.56 ± 0.03	29.12 ± 1.57	817.19 ± 1.60	^{115}In d	17.80	818.70 ± 0.05
	0.56 ± 0.03	32.92 ± 2.16	876.87 ± 1.16	^{58}Ni	0.23	877.97 ± 0.05
	0.56 ± 0.03	26.40 ± 1.12	1505.15 ± 2.75	^{115}In d	15.50	1507.40 ± 0.05

Table 4: *In-resonance peaks analysis of the leaded bronze. In grey we highlighted the contribution emerging from the background after cuts in the indicated TOF ranges.*

4. Conclusions

In this paper we explored the potential of the new time-resolved prompt gamma activation analysis on INES beamline at ISIS Spallation Neutron and Muon Source in Oxfordshire, UK. This technique allows to reveal the photon energy emitted by the sample during irradiation, as a function of time of flight. A protocol for analysis was developed and tested on certified metal samples.

The data analysis carried out using ad hoc algorithms developed through ROOT software allowed to introduce the time component in a proactive way, aiming at exploit the time information to increase the accuracy of the analysis for major and minor elements. The technique has proven to be promising to provide a good qualitative identification of the elements within the standard samples and a good quantification of each element that has been compared to the certified values. The only significant discrepancy was noted in the quantification of zinc, mainly due to the background subtraction process. This issue is being investigated by the application of Compton suppression chain and coincidence electronics using YAP detectors, but it is noted that this problem is not relevant for the analysis of most prehistoric copper alloys, which do not contain this element in significant concentrations.

This work aimed at providing a procedure to integrate the quantitative analysis of the elements identified within a sample improving the capability of PGAA technique at spallation sources. Exploiting

*Prof. Roberto Senesi: roberto.senesi@uniroma2.it

the time component, peculiar of these neutron sources, helped increase the sensitivity to detect and quantify minor elements in two standards. This paper demonstrates that T-PGAA technique and the software for the data analysis is ready to be used on real case studies such as the non-invasive characterisation of prehistoric Cu-based objects. Furthermore, our results show that PGAA, successfully used at reactors, can be integrated as a complementary technique at spallation sources on beamlines dedicated to different techniques, to provide a simultaneous and non-invasive characterisation.
In conclusion T-PGAA and the data analysis software developed using ROOT software and tailored for the technique, are demonstrated to be valid and applicable for non-invasive bulk chemical analysis of metal objects at an isotopic level, providing qualitative and quantitative information on major and trace elements. The technique therefore offers significant potential in archaeological science and materials characterisation more generally

Acknowledgements
This work is partially supported by the CNR-STFC agreement (2014-2020) concerning collaboration in scientific research at the ISIS pulsed Neutron and Muon Source. We thank Dr Angelo Agostino, Università di Torino, for providing the metal standard samples used in this paper. We are grateful to Dr Alfio Pappalardo, INFN, for supporting with the technique setup. GF, RS, LA and CA would like to acknowledge the support of the Centro FERMI within the Tecniche Neutroniche per Archeologia e Analisi Forense (TNAAF) project.

References

[1] N. Kardjilov and G. Festa, Neutron Methods for Archaeology and Cultural Heritage, Springer International Publishing AG (2016).

[2] Zs. Révay, “Determining elemental composition using prompt gamma activation analysis”, Anal. Chem. 82, 6851-6859 (2009).

[3] Y. Toh, M. Ebihara, A. Kimura, S. Nakamura, H. Harada, K. Y. Hara, M. Koizumi, F. Kitatani and K. Furutaka, Synergistic Effect of Combining Two Nondestructive Analytical Methods for Multielemental Analysis, Analytical Chemistry 86, 12030−12036 (2014).

[4] G. Festa, L. Arcidiacono, A. Pappalardo, T. Minniti, C. Cazzaniga, A. Scherillo, C. Andreani, R. Senesi, "Isotope identification capabilities using time resolved prompt gamma emission from epithermal neutrons", Journal of Instrumentation 11 C03060 (2016).

[5] G. Festa, C. Andreani, L. Arcidiacono, F. Grazzi and R. Senesi, Neutron Diffraction and (n,γ)-based techniques for Cultural Heritage in “Nanotechnologies and Nanomaterials for Diagnostic, Conservation and Restoration of Cultural Heritage”, G. Lazzara and R. Fakhrullin, Elsevier, https://doi.org/10.1016/B978-0-12-813910-3.00004-5 (2018).

[6] W. Reimers, A. R. Pyzalla, A. K. Schreyer, H. Clemens, “Neutrons and Synchrotron Radiation in Engineering Materials Science: From Fundamentals to Material and Component Characterization”, Wiley-VCH Verlag (2008).

[7] F. Grazzi, F. Civita, A. Williams, A. Scherillo, E. Barzagli, L. Bartoli, D. Edge, M. Zoppi, “Ancient and historic steel in Japan, India and Europe, a non-invasive comparative study using thermal neutron diffraction”, Analytical and bioanalytical chemistry, 400/5, 1493-1500 (2011).

*Prof. Roberto Senesi: roberto.senesi@uniroma2.it

[8] G. Festa, T. Minniti, L. Arcidiacono, M. Borla, D. Di Martino, F. Facchetti, E. Ferraris, V. Turina, W. Kockelmann, J. Kelleher, R. Senesi, C. Greco and C. Andreani. Egyptian grave goods of Kha and Merit studied by neutron and gamma techniques. Angew. Chem. Int. Ed. 57, 1 – 6 (2018).

[9] H. Postma, L. Amkreutz, D. Fontijn, H. Kamermans, W. Kockelmann, P. Schillebeeckx, D. Visser, "Neutron-based analyses of three Bronze Age metal objects: a closer look at the Buggenum, Jutphaas and Escharen artefacts", Analecta Praehistorica Leidensia, P.J.R. Modderman Stichting ed. (2017).

[10] T. Belgya, Z. Kis, L. Szentmiklósi, P. Kudejova, R. Schulze, T. Materna, G. Festa, P. A. Caroppi, C. Andreani, "First elemental imaging experiment on a combined PGAI and NT set up at the Budapest Research Reactor, Journal of Radioanalytical and Nuclear Chemistry, 278, No. 3, 751-754 (2008).

[11] I. S. Anderson, C. Andreani, J. Carpenter, G. Festa, G. Gorini, C.-K Loong, R. Senesi, "Research Opportunities with Compact Accelerator-Driven Neutron Sources", Physics Reports 654, 1–58 (2016).

[12] R.W. Peelle, F.C. Maienschein, "Spectrum of photons emitted in coincidence with fission of ^{235}U by thermal neutrons", Phys. Rev. C 3 (1) 373–390 (1971).

[13] H. Postma, M. Blaauw, P. Schillebeeckx, G. Lobo, R.B. Halbertsma, A.J. Nijboer, "Non-destructive elemental analysis of copper-alloy artefacts with epithermal neutron-resonance capture", Czechoslovak Journal of Physics 53, 1, 233-240 (2003).

[14] A. Pietropaolo, G. Gorini, G. Festa, E. Reali, F. Grazzi, E. Schooneveld, "A neutron resonance capture analysis experimental station at the ISIS Spallation Source", Applied Spectroscopy, 64, 9, 1068-1071 (2010).

[15] X-Ray Fluorescence Spectrometry, 2nd Edition, Ron Jenkins, Wiley, ISBN: 978-0-471-29942-4, 1999

[16] S. Imberti, W. Kockelmann, M. Celli, F. Grazzi, M. Zoppi, A. Botti, A. Sodo, et al., "Neutron diffractometer INES for quantitative phase analysis of archaeological objects", Meas. Sci. Technol. 19 034003 (2008).

[17] MBH Analytical Ltd web site: http://mbh.co.uk, access date: 29/07/2019

[18] A. Pietropaolo, G. Festa, F. Grazzi, E. Barzagli, A. Scherillo, E. M. Schooneveld, "A multitask neutron beam line for spallation neutron sources", Europhysics Letters, 95, 48007 (2011).

[19] ORTEC website: https://www.ortec-online.com, access date: 29/07/2019

[20] R. Brun and F. Rademakers, "ROOT - an object oriented data analysis framework" Proceedings AIHENP'96 Workshop Lausanne Nucl Inst and Meth. in Physics A 389 (1997).

[21] Zs. Revay, T. Belgya, P.P. Ember, G.L. Molnar, "Recent developments in HYPERMET PC" Journal of Radioanalytical and Nuclear Chemistry 248 (2000).

[22] A. Parmentier, L. Arcidiacono, R. Senesi, G. Romanelli, C. Andreani, J. Moir, G. Festa, "Absolute efficiency calibration of a coaxial HPGe detector for quantitative PGAA and T-PGAA" Journal of Physics: Conference Series, 1055 (1), 012010 (2018).

*Prof. Roberto Senesi: roberto.senesi@uniroma2.it

[23] G. W. Phillips and K. W. Marlow, "Program HYPERMET for automatic analysis of gamma-ray spectra from germanium detectors", Nucl. Instrum. Methods 72 (1976).

[24] G. Molnár, “Handbook of Prompt Gamma Activation Analysis - with Neutron Beams”, Springer (2004).

[25] IAEA - Thermal Neutron Capture γ's (CapGam): https://www-nds.iaea.org/capgam/index.htmlx, access date: 29/07/2019

[26] L. Arcidiacono, A. Parmentier, G. Festa, M. Martinón-Torres, C. Andreani, R. Senesi, “Validation of a new data-analysis software for multiple-peak analysis of γ spectra at ISIS pulsed Neutron and Muon Source”, Nuclear Inst. and Methods in Phisics Research, A 938, 51-55 (2019).

[27] E. Fairstein, S. Wagner, "IEEE standard test procedures for germanium gamma-ray detectors" IEEE std (1996).

[28] B. Fazekas, Zs. Rvay, J. Ostor, T. Belgya, G. Molnar, A. Simonits, "A new method for determination of gamma-ray spectrometer non-linearity", NIM A (1999).

[29] Z. Kis, 196 B. Fazekas, J. Ostor, Z. Rvay, T. Belgya, G.L. Molnar, L. Koltay, "Comparison of efficiency functions for Ge gamma-ray detectors in a wide energy range", NIM A (1998).

*Prof. Roberto Senesi: roberto.senesi@uniroma2.it